Hard x-ray photoelectron spectroscopy of the metal-insulator transition in $LiRh_2O_4$

Y. Nakatsu,[1] A. Sekiyama,[1,3] S. Imada,[1,*] Y. Okamoto,[2,†] S. Niitaka,[2] H. Takagi,[2] A. Higashiya,[3,‡] M. Yabashi,[3] K. Tamasaku,[3] T. Ishikawa,[3] and S. Suga[1,3]

[1]*Division of Materials Physics, Graduate School of Engineering Science, Osaka University, Toyonaka, Osaka 560-8531, Japan*

[2]*RIKEN, Wako, Saitama 351-0198, Japan*

[3]*SPring-8/RIKEN, Sayo, Hyogo 679-5148, Japan*

(Received 15 October 2010; revised manuscript received 3 February 2011; published 14 March 2011)

We have applied hard x-ray photoelectron spectroscopy to $LiRh_2O_4$ to study its bulk electronic structures. $LiRh_2O_4$ shows the metal-insulator transition (MIT) at 170 K when the temperature is decreased via an intermediate phase, which appears below 230 K and is ascribed to the band Jahn-Teller instability. Clear spectral changes are observed across the MIT for both the valence band near the Fermi level (E_F) and the Rh 3*d* core state. Their slight spectral changes are also observed across 230 K, induced by the orbital ordering and the slight change of the screening by conduction electrons. The linear polarization dependence of the spectra was measured for the O 2*s* and valence-band states. The contribution of the Rh 5*s* state hybridized with the O 2*p* states in the valence band is semiquantitatively evaluated.

DOI: 10.1103/PhysRevB.83.115120 PACS number(s): 71.30.+h, 79.60.−i

I. INTRODUCTION

Elucidation of the mechanism of the metal-insulator transition (MIT) has been one of the major subjects in solid-state physics.[1,2] Among various transition-metal oxides with MIT, the spinel with the chemical formula of AB_2O_4 attracts wide interest. The *B* site sublattice corresponds to the pyrochlore lattice, where such phenomena as the quantum-spin liquid, lattice distortion, and orbital ordering are often discussed.[3] Charge frustration is also discussed in the spinel Fe_3O_4 ($Fe_1Fe_2O_4$) with equivalent amounts of Fe^{2+} and Fe^{3+} on the *B* site. Spinel crystals such as $CuIr_2S_4$ and $MgTi_2O_4$ show a MIT[4–9] accompanied by the crystal distortion from the cubic to tetragonal structures. In fact, additional distortion is added to a tetragonal distortion in $CuIr_2S_4$, resulting in a quasitetragonal or a triclinic structure. The newly synthesized spinel-type compound $LiRh_2O_4$ shows, however, a slightly more complicated MIT.[3,10] $LiRh_2O_4$ is found to be a mixed-valent spinel oxide with equal amounts of $Rh^{3+}(4d^6, S = 0)$ and $Rh^{4+}(4d^5, S = 1/2)$. Then Rh^{4+} has one hole in the sixfold degenerate t_{2g} orbital.[3] The distinctive feature of MIT in $LiRh_2O_4$ is the two-step MIT process via the intermediate phase. A transition from an orbital-disordered metal phase to an orbital-ordered metal phase occurs at 230 K. The orbital ordering in the latter phase in the metal of $LiRh_2O_4$ is argued to take place between the single *xy* band and doubly degenerate *yz*, *zx* bands with the t_{2g}character. The band Jahn-Teller instability is one of the candidates for this transition because of the intrinsic band instability of the 0.5-hole-doped t_{2g} band in $LiRh_2O_4$.[3] Below 170 K a charge-ordered valence-bond solid (VBS) is formed, where the holes are confined within the quasi-one-dimensional *xy* band.

In a mixed-valence spinel, $CuIr_2S_4$, a charge ordering and MIT appear through the cooling process. The orbitally driven Peierls transition[4] is suggested to be their origin. On the orbital ordering, the tetragonal distortion removes the triple degeneracy of the t_{2g} band, stabilizing the *yz* and *zx* states and destabilizing the *xy* state. Then the *yz* and *zx* orbitals are occupied with four electrons and the *xy* band accommodates only 1.5 electrons. This highly extended *xy* state, due to the shrinkage of the lattice constant *a* by the tetragonal distortion, facilitates the dominant hopping along the [1,1,0] and [1,−1,0] directions, forming a one-dimensional *xy* band in $CuIr_2S_4$. On cooling, Ir^{4+} makes dimers with neighboring Ir^{4+}.[11] The charge-density wave (CDW) is formed by the dimer formation through these *xy* chains, inducing an orbitally driven metal-to-insulator transition.

Although the lattice distortion was commonly observed in both $LiRh_2O_4$ and $CuIr_2S_4$, the details of the lattice distortion and charge ordering are slightly different in between,[11,12] requiring a careful experimental approach. In order to discuss detailed differences of the MIT between $LiRh_2O_4$ and $CuIr_2S_4$, bulk-sensitive and high-resolution photoelectron spectroscopy is definitely required. Since differences between surface and bulk electronic structures are well known in strongly correlated electron systems by means of high-resolution soft x-ray photoelectron spectroscopy,[13,14] hard x-ray photoelectron spectroscopy (HAXPES) is mandatory for this purpose.[15–17] Although we have already reported on the temperature dependence of the HAXPES in the vicinity of the Fermi level,[3] the changes of band structures of the whole valence-band and core-level spectra through these three phases are still not yet fully studied. In addition, the contribution of the Rh 5*s* state in the valence band is studied in this work by use of the polarization-dependent HAXPES. Thus by use of the state-of-the-art HAXPES techniques, the bulk electronic structures and their changes on phase transitions are fully experimentally clarified.

II. EXPERIMENTAL

In order to study the roles of the orbital and charge orderings in both intermediate and insulator phases, we measured the whole valence band and Rh core level by means of the bulk-sensitive HAXPES. HAXPES measurements were performed at $h\nu = 8180$ eV on the beam line BL19LXU of SPring-8 by using an MB Scientific A1-HE spectrometer. The total energy resolution was set to 250 meV for the measurement of the Rh 3*d* core and valence-band spectra. The detailed studies near

the Fermi level (E_F) were performed with a total resolution of 150 meV. Polycrystalline $LiRh_2O_4$ samples were synthesized by means of solid-state reaction.[3] Clean surfaces were obtained by *in situ* fracturing. We performed the HAXPES measurements at 250 K (metal phase), 210 K (intermediate phase), and 160 K (insulating phase). The light was horizontally incident on the sample, which was vertically positioned. The light incidence angle was set to ∼60° from the surface normal and the near normal emission of photoelectrons was measured in the horizontal plane. In addition to the HAXPES measurements with the horizontally polarized light from the 27-m-long planar undulator, we also performed the measurements with the vertically polarized light by using a diamond x-ray phase shifter. This technique is rather powerful in separating the electronic structures with different symmetries. Usually plural orbitals are highly mixed in the valence band and it is not straightforward to clarify their relative spectral weight. However, a characteristic angular distribution is expected for the individual orbitals with different symmetries in the photoemission process.[18] Then the excitation probability of s orbitals becomes much less than those of the p or d orbitals, when we switch the polarization of the incident x ray from the horizontal polarization (π-polarization configuration) to the vertical polarization (σ-polarization configuration).[19] We utilize such behavior to separate individual orbitals. The transmittance of photons of ∼35.6% was realized in our case for the vertically polarized x ray when compared with the photon flux without the diamond x-ray phase shifter. The degree of the linear polarization was checked by the intensities of the lights scattered by a polyimide film. Near E_F the Rh 4d and O 2p orbitals play very important roles in $LiRh_2O_4$. However, the Rh 5s orbital has a much higher photoionization cross section than the O 2p orbitals at $h\nu$ = 8 keV for the incidence of the horizontally polarized x ray. The s-symmetry state can be well suppressed by changing the linear polarization of the excitation light to the vertical direction. On this occasion, the photoemission intensity from the p and d orbitals is less dependent on P_L,[18] the degree of the linear polarization, which is defined by the following:

$$P_L = (I_x - I_y)/(I_x + I_y). \quad (1)$$

Here I_x and I_y stand for the intensities of the horizontally and vertically polarized light, respectively. $P_L = 1.0$ (-1.0) corresponds to the completely horizontal (vertical) polarization.

III. RESULTS AND DISCUSSION

The dependence of the HAXPES spectra ($h\nu$ = 8180 eV) on the incident light polarization is shown in Fig. 1. For the vertically polarized x-ray HAXPES measurements, we succeeded in realizing a high polarization of $P_L = -0.82$, where the weight of the horizontally polarized component is <10%. The O 2s peak near the binding energy (E_B) of 20 eV is clearly suppressed for $P_L = -0.82$ (Fig. 1). One can evaluate the spectrum for $P_L = -1.0$ by comparing the two spectra for $P_L = 1.0$ and -0.82. As expected, the O 2s peak is further weakened for $P_L = -1.0$. For the valence band, one notices that the structures B and C are decreased relative to A when the polarization is changed from $P_L = 1.0$ to -0.82. Then the

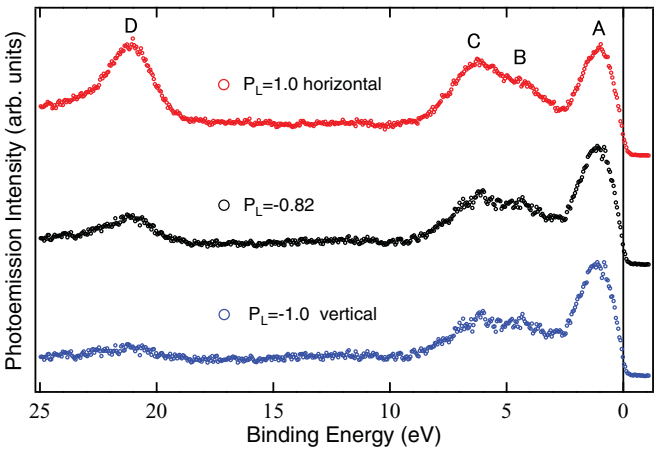

FIG. 1. (Color online) Valence-band HAXPES spectra of $LiRh_2O_4$ taken at $h\nu$ = 8180 eV and 250 K. $P_L = 1.0$ and $P_L = -0.82$ spectra were obtained by horizontally and vertically polarized x rays, respectively. The $P_L = -1.0$ spectrum is derived from the two spectra for $P_L = 1.0$ and $P_L = -0.82$[M1].

valence-band spectra for $P_L = 1.0$ and -1.0 are tentatively normalized at the peak near $E_B = 1.0$ eV, as shown in Fig. 2.

It is known that the suppression of the p states for the vertically polarized x ray is much less than that for s states.[18,19] Consequently one may think of a possibility as the weakened structures B and C for $P_L = -1.0$ are due to the O 2p states. However, the photoionization cross section of the O 2p state is 100 times weaker than that of the Rh 4d state according to the calculated photoionization cross section.[20] So the B and C components for $P_L = -1.0$ represent the Rh 4d dominated component. Of course the Rh 4d states give the prominent peak A near E_F. Thus the broad structures B and C above E_B = 2 eV are ascribed to the O 2p-Rh 4d bonding states in the

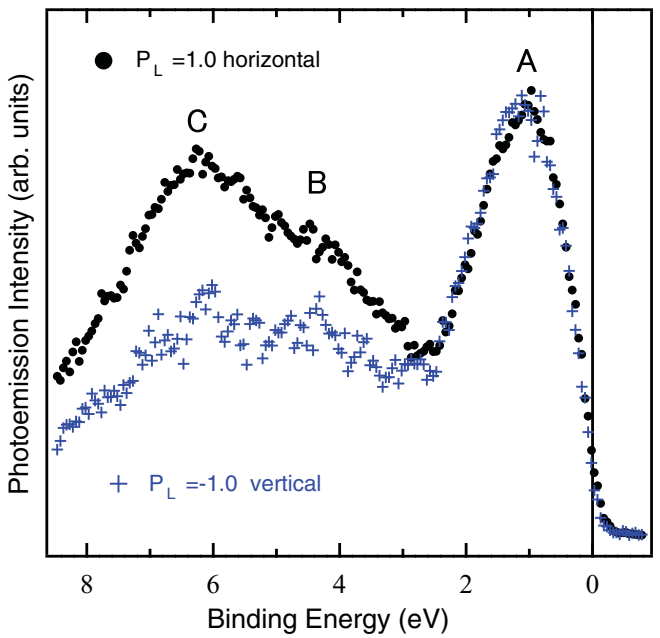

FIG. 2. (Color online) Horizontally polarized ($P_L = 1.0$) and vertically polarized ($P_L = -1.0$) valence-band HAXPES spectra of $LiRh_2O_4$ taken at 250 K.

$P_L = -1.0$ spectrum. The difference between the two spectra for $P_L = 1.0$ and -1.0 is then ascribed to the Rh 5*s* contribution. Namely, the subsidence at approximately $E_B = 6$ eV may be due to the suppression of the Rh 5*s* state hybridized with the O 2*p* state.

Before studying the spectral changes with temperature, the structural changes with temperature were studied. According to the powder x-ray diffraction,[3] $LiRh_2O_4$ has a cubic spinel structure in the metal phase at room temperature with equivalent Rh sites. The diffraction pattern in the intermediate phase between 270 and 170 K shows the tetragonal structure, and the cubic-tetragonal transition can be understood as due to the simple elongation of the cubic spinel structure along [001]. The x-ray diffraction pattern in the insulating phase below 170 K shows the orthorhombic structure. According to the electron diffraction patterns, a complicated lattice distortion and resultant lowering of symmetry with charge ordering are suggested.[3]

Since there are almost no significant spectral changes with temperature in the valence band above $E_B = 4$ eV, we focus on the behavior in the E_B region below 3 eV. Figure 3(a) shows the $P_L = 1.0$ spectra measured at 250, 210, and 160 K. The intensity at E_F is finite at 250 K (metal phase) but a band gap is clearly seen at 160 K (insulating phase), confirming that the transition from the metal to the insulator has occurred with decreasing temperature. Although the spectral difference between 250 and 160 K in $LiRh_2O_4$ is apparently similar to that in the x-ray photoelectron spectra (XPS) of $CuIr_2S_4$ across 230 K,[21] there is a clear difference in between. Namely, the spectrum at 210 K in $LiRh_2O_4$ is different from the spectra at both 250 and 160 K. Though the spectrum represents the metallic feature at 210 K, its intensity at E_F is slightly decreased compared to what it is at 250 K [Fig. 3(b)], suggesting the presence of the intermediate phase with metallic character. Moreover, the change of the spectral shape in the whole energy range in Fig. 3(a) is in contrast to the rigid shift observed in $CuIr_2S_4$. It is noticed that the peak height near 1 eV increases gradually as the temperature is decreased from 250 to 160 K. On the other hand, the intensity in the region between E_F and $E_B = 0.5$ eV is noticeably decreased through 250, 210, and 160 K, as shown in Fig. 3(b). As explained previously, the tetragonal distortion removes the degeneracy of the t_{2g} state into fully occupied and degenerate *yz* and *zx* states and a partially occupied *xy* state below 230 K in accordance with the band Jahn-Teller effects. In this sense, the peak near 1.0 eV below 230 K is most probably due to the *yz* and *zx* states. With a further decrease in temperature, a band gap of ~150–200 meV is observed from the clear shift of the low E_B threshold across the MIT temperature of 170 K. Because the dimerization along the *xy* chains induces the Peierls transition, the *xy* state seems to be located in the vicinity of E_F above 170 K and is responsible for the drastic spectral change between 210 and 160 K. This spectral component is transferred to the enhanced peak near 1.2 eV below 170 K.

Here one may ask about the possible influence of the photoelectron recoil effect, which is already revealed in LiV_2O_4.[22] In $LiRh_2O_4$, the recoil effect could not be confirmed by the Li 1*s* core spectrum, which is not well resolved as the photoionization cross section of the Rh 4*p* core state is two orders of magnitude larger than that of the Li 1*s*

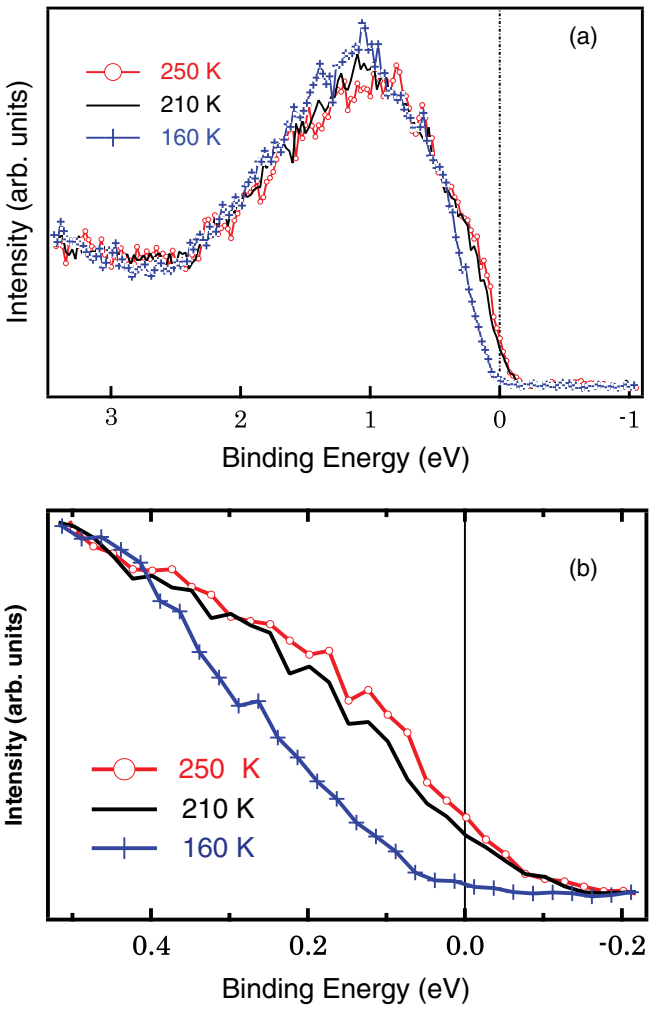

FIG. 3. (Color online) (a) Valence-band HAXPES spectra of $LiRh_2O_4$ excited by the horizontally polarized light ($P_L = 1.0$) taken at 250, 210, and 160 K. The spectra are normalized by the integrated intensity up to 3.5 eV. (b) The same spectra expanded up to 0.5 eV.

state. For the valence band in LiV_2O_4 the recoil effect was clarified[22] because of the comparable photoionization cross sections between the O 2*p* and V 3*d* states, for which the single nucleus recoil shifts of ~250 and ~60 meV were expected. However, the photoionization cross section of the Rh 4*d* state is two orders of magnitude larger than that of the O 2*p* state in $LiRh_2O_4$.[20] Even though the single nucleus recoil effect takes place for the valence band in this material, its magnitude is dominated by the possible recoil shift of the Rh 4*d* state, which is ~20 meV. Then the photoelectron recoil effect for the valence band is almost negligible in $LiRh_2O_4$ within the present resolution.

Figure 4(a) shows the Rh 3*d* core-level $P_L = 1.0$ spectra taken at 250 K. Some faint structures shown with the vertical bar ~10 eV above the main peak are most probably interpreted as the charge-transfer (CT) satellite screened by the O 2*p* ligand band.[23] Figure 4(b) shows the temperature dependence of the Rh $3d_{5/2}$ core-level spectra normalized by the integrated intensity of both Rh $3d_{5/2}$ and $3d_{3/2}$ components, which change dramatically through the MIT at 170 K. Namely, the

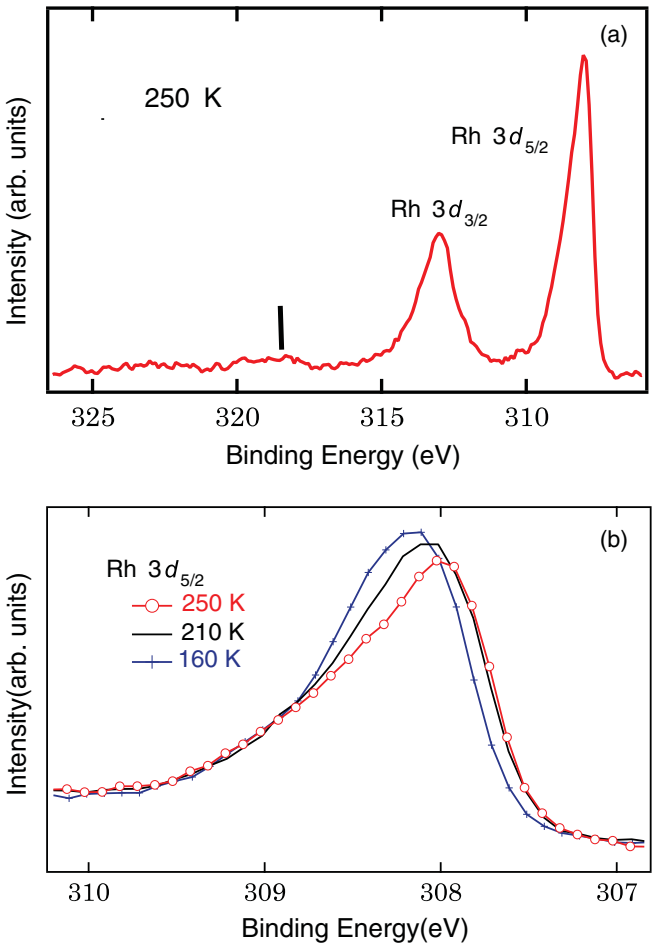

FIG. 4. (Color online) (a) Rh 3*d* HAXPES spectra ($P_L = 1.0$) of $LiRh_2O_4$ at 250 K. (b) Rh $3d_{5/2}$ HAXPES spectra ($P_L = 1.0$) taken at 250, 210, and 160 K.

low-energy threshold part in the metal phase is very suppressed in the insulator phase. In addition, a slight but noticeable change is also observed through 230 K on the higher E_B side of the peak between the metal and the intermediate phases.

Now the spectral shapes are analyzed by considering multicomponents in Fig. 5. Any surface components can be excluded by the bulk sensitivity of HAXPES.[15–17] Although the spectrum at 160 K is well reproduced by two components with Gaussian spectral shapes corresponding to the Rh^{3+} and Rh^{4+} states,[21] the spectra at 250 and 210 K are not well reproduced without considering the third component located at the lowest E_B. This additional structure is interpreted as due to the long-range metallic screening (or well-screened structure).[15] This well-screened feature decreases in the intermediate phase and finally disappears in the insulator phase. This result is fully consistent with the reduction of the photoemission intensity at E_F in Fig. 3(b). The two components at higher E_B are then interpreted as poorly screened peaks. The poorly screened peak with smaller E_B (blue line) increases in the intermediate phase compared to that in the metal phases at 250 K. This increase may be correlated with the decreased photoemission intensity at E_F and ascribed to the decreased screening by free

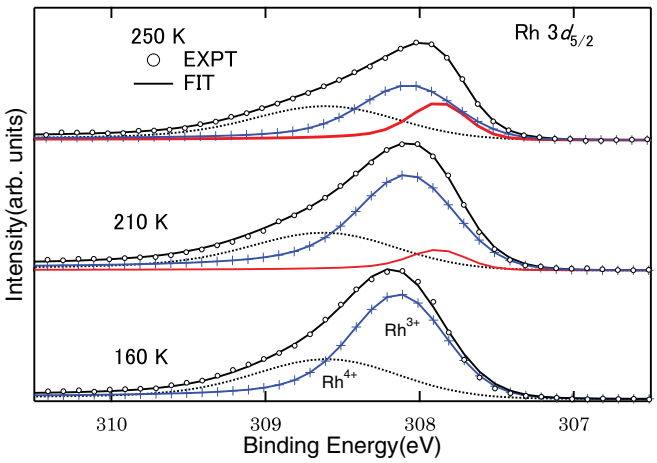

FIG. 5. (Color online) Rh $3d_{5/2}$ HAXPES data (open circles) of $LiRh_2O_4$ ($P_L = 1.0$), at 250, 210, and 160 K. Lower curves show the individual components (solid line with +: Rh^{3+} component; dotted line: Rh^{4+} component; solid line: well-screened component), whose sum is given by the solid curves through the experimental data.

carriers. Only the *xy*-band electrons can screen core holes in the intermediate phase, resulting in the decrease of the well-screened feature. The increase of the poorly screened component (blue solid line through the + marks) in the intermediate phase coincides with the reduction of the well-screened peak. These results, combined with the two-step phase transition, have revealed that the origin of MIT in $LiRh_2O_4$ is clearly different from that in $CuIr_2S_4$.

IV. CONCLUSION

We have performed high-resolution bulk-sensitive HAXPES studies of $LiRh_2O_4$ including the incidence light polarization dependence. On changing the sample temperature, clear spectral changes of the valence-band spectra are observed near E_F on the metal-insulator transition at 170 K that are associated with the charge ordering. Small but noticeable spectral changes are observed across 230 K in accordance with the orbital ordering. The intermediate phase between 230 and 170 K is confirmed to also be a metal phase. Clear spectral changes are observed as well for the Rh 3*d* core-level spectra with high enough bulk sensitivity. The results are in full agreement with the spectral changes of the valence band near E_F. The contribution of the Rh 5*s* states hybridized with the O 2*p* states in the valence band is semiquantitatively evaluated by the linear polarization dependence of the HAXPES spectra. Additionally, the negligible recoil effects near E_F are consistent with the predominance of the Rh 4*d* states over the O 2*p* states near E_F in HAXPES, which provides a very low photoionization cross section to the O 2*p* states relative to the Rh 4*d* states. Thus the potential of high-resolution HAXPES to study bulk electronic structures in solids is fully demonstrated.

ACKNOWLEDGMENTS

The authors are much obliged to the support by a Grant-in-Aid for Scientific Research (18104007, 15GS0123, 18684015, 21740229, 21340101) from MEXT, Japan.

*Present address: Department of Physical Sciences, College of Science and Engineering, Ritsumeikan University, Kusatsu, Shiga 525-8577, Japan.
†Present address: Institute for Solid State Physics, The University of Tokyo, Kashiwanoha 5-1-5, Kashiwa 277-8581, Japan.
‡Present address: Industrial Technology Center of Wakayama Prefecture, Wakayama 649-6262, Japan.

[1] J. Zaanen, G. A. Sawatzky, and J. W. Allen, Phys. Rev. Lett. **55**, 418 (1985).
[2] M. Taguchi, A. Chainani, N. Kamakura, K. Horiba, Y. Takata, M. Yabashi, K. Tamasaku, Y. Nishino, D. Miwa, T. Ishikawa, S. Shin, E. Ikenaga, T. Yokoya, K. Kobayashi, T. Mochiku, K. Hirata, and K. Motoya, Phys. Rev. B **71**, 155102 (2005).
[3] Y. Okamoto, S. Niitaka, M. Uchida, T. Waki, M. Takigawa, Y. Nakatsu, A. Sekiyama, S. Suga, R. Arita, and H. Takagi, Phys. Rev. Lett. **101**, 086404 (2008).
[4] D. I. Khomskii and T. Mizokawa, Phys. Rev. Lett. **94**, 156402 (2005).
[5] K. Takubo, S. Hirata, J.-Y. Son, J. W. Quilty, T. Mizokawa, N. Matsumoto, and S. Nagata, Phys. Rev. Lett. **95**, 246401 (2005).
[6] E. Z. Kurmaev, V. R. Galakhov, D. A. Zatsepin, V. A. Trofimova, S. Stadler, D. L. Ederer, M. M. Grush, T. A. Callcott, J. Matsuno, A. Fujimori, and S. Nagata, Solid State Commun. **108**, 235 (1998).
[7] M. Isobe and Y. Ueda, J. Phys. Soc. Jpn. **71**, 1848 (2002).
[8] T. Furubayashi, T. Matsumoto, T. Hagino, and S. Nagata, J. Phys. Soc. Jpn. **63**, 3333 (1994).
[9] K. Matsuno, T. Katsufuji, S. Mori, Y. Moritomo, A. Machida, E. Nishibori, M. Takata, M. Sakata, N. Yamamoto, and H. Takagi, J. Phys. Soc. Jpn. **70**, 1456 (2001).
[10] R. Arita, K. Kuroki, K. Held, A.V. Lukoyanov, S. Skornyakov, and V. I. Anisimov, Phys. Rev. B **78**, 115121 (2008).
[11] P. Radaelli, Y. Horibe, M. Gutmann, H. Ishibashi, C. Chen, R. Ibberson, Y. Koyama, Y. Hor, V. Kiryukhin, and S. Cheong, Nature (London) **416**, 155 (2002).
[12] K. Takubo, S. Hirai, J. Y. Son, J. W. Quilty, T. Mizokawa, N. Matsumoto, and S. Nagata, Phys. Rev. Lett. **95**, 246401 (2005).
[13] A. Sekiyama, T. Iwasaki, K. Matsuda, Y. Saitoh, Y. Onuki, and S. Suga, Nature (London) **403**, 396 (2000).
[14] S. Suga, A. Sekiyama, S. Imada, A. Shigemoto, A. Yamasaki, M. Tsunekawa, C. Dallera, L. Braicovich, T. L. Lee, O. Sakai, T. Ebihara, and Y. Onuki, J. Phys. Soc. Jpn. **74**, 2880 (2005).
[15] K. Horiba, M. Taguchi, A. Chainani, Y. Takata, E. Ikenaga, D. Miwa, Y. Nishino, K. Tamasaku, M. Awaji, A. Takeuchi, M. Yabashi, H. Namatame, M. Taniguchi, H. Kumigashira, M. Oshima, M. Lippmaa, M. Kawasaki, H. Koinuma, K. Kobayashi, T. Ishikawa, and S. Shin, Phys. Rev. Lett. **93**, 236401 (2004)
[16] A. Yamasaki, S. Imada, H. Higashimichi, H. Fujiwara, T. Saita, T. Miyamachi, A. Sekiyama, H. Sugawara, D. Kikuchi, H. Sato, A. Higashiya, M. Yabashi, K. Tamasaku, D. Miwa, T. Ishikawa, and S. Suga, Phys. Rev. Lett. **98**, 156402 (2007).
[17] S. Suga and A. Sekiyama, Europhys. J. **169**, 227 (2009).
[18] A. Sekiyama, J. Yamaguchi, A. Higashiya, M. Obara, H. Sugiyama, M. Y. Kimura, S. Suga, S. Imada, I. A. Nekrasov, M. Yabashi, K. Tamasaku, and T. Ishikawa, New J. Phys. **12**, 043045 (2010).
[19] M. B. Trzhaskovskaya, V. K. Nikulin, V. I. Nefedov, and V. G. Yarzhemsky, At. Data Nucl. Data Tables **92**, 245 (2006).
[20] J. J. Yeh and I. Lindau, At. Data Nucl. Data Tables **32**, 1 (1985).
[21] H. J. Noh, E. J. Cho, H. D. Kim, J. Y. Kim, C. H. Min, B. G. Park, and S. W. Cheong, Phys. Rev. B **76**, 233106 (2007).
[22] S. Suga, A. Sekiyama, H. Fujiwara, Y. Nakatsu, T. Miyamachi, S. Imada, P. Baltzer, S. Niitaka, H. Takagi, K. Yoshimura, M. Yabashi, K. Tamasaku, A. Higashiya, and T. Ishikawa, New J. Phys. **11**, 073025 (2009).
[23] S. Suga, A. Sekiyama, S. Imada, T. Miyamachi, H. Fujiwara, A. Yamasaki, K. Yoshimura, K. Okada, M. Yabashi, D. Miwa, K. Tamasaku, A. Higashiya, and T. Ishikawa, New J. Phys. **11**, 103015 (2009).